

Interface solitons in two-dimensional photonic lattices

Mario I. Molina

Departamento de Física, Facultad de Ciencias,
Universidad de Chile, Casilla 653, Santiago, Chile

Yuri S. Kivshar

Nonlinear Physics Center, Research School of Physical Sciences and Engineering,
Australian National University, Canberra ACT 0200, Australia

We analyze localization of light at the interface separating square and hexagonal photonic lattices, as recently realized experimentally in two-dimensional laser-written waveguide arrays in silica glass with self-focusing nonlinearity [A. Szameit *et al.*, Opt. Lett. **33**, 663 (2008)]. We reveal the conditions for the existence of *linear* and *nonlinear* surface states substantially influenced by the lattice topology, and study the effect of the different symmetries and couplings on the stability of two-dimensional interface solitons.

© 2018 Optical Society of America

OCIS codes: 190.4420; 190.5530; 190.5940

Theoretical results on the existence of novel types of discrete surface solitons localized in the corners or at the edges of two-dimensional photonic lattices [1, 2, 3] have been recently confirmed by the experimental observation of two-dimensional surface solitons in optically-induced photonic lattices [4] and two-dimensional waveguide arrays laser-written in fused silica [5, 6]. These two-dimensional nonlinear surface modes demonstrate novel features in comparison with their counterparts in truncated one-dimensional waveguide arrays [7, 8, 9]. In particular, in a sharp contrast to one-dimensional discrete surface solitons, the mode threshold is lower at the surface than in a bulk making the mode excitation easier [2].

Recently, Szameit *et al.* [10] reported on the first experimental observation of two-dimensional interface solitons, i.e. spatial optical solitons generated at the interface separating square and hexagonal optical lattices with different refractive index modulation depths. Such two-dimensional interface solitons feature *asymmetric shapes*, while differences in array properties and lattice topology strongly affect the threshold power for soliton existence and excitation as well as soliton stability.

In this Letter, we study this problem analytically in a more general setting and analyze localization of light at the interface separating two lattices of different symmetries in the framework of the two-dimensional discrete nonlinear model. We assume that the interface is created between the square and hexagonal two-dimensional optical lattices, similar to the case studied earlier [10], but we assume the coupling parameters to be different and study the effect of different symmetries and lattice topology, as well as the coupling strength of the interface on the existence and stability of both *linear* and *nonlinear* surface states. In particular, we determine the conditions for the thresholdless surface states (linear surface modes) that appear due to the breaking of the lattice topology, and also study the nonlinear localization and generation

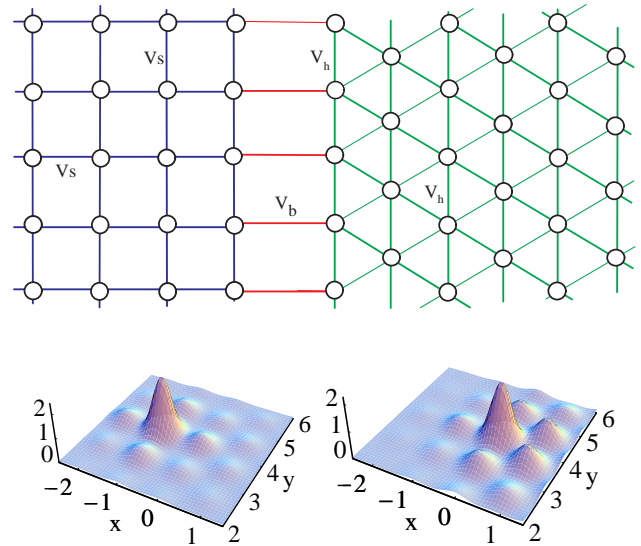


Fig. 1. (Color online) Top: Sketch of a square-hexagonal photonic lattice. Bottom: Examples of low-order nonlinear interface mode centered (left) on the site belonging to the boundary of the square lattice (which ends at $x = -1$), and (right) on the site belonging to the boundary of the hexagonal lattice (which starts at $x = 0$).

of two-dimensional interface solitons.

We consider a semi-infinite two-dimensional optical lattice created by a square array of optical waveguides joined to the other semi-infinite but hexagonal lattice along a straight boundary, as shown in Fig. 1 (top).

In the framework of the coupled-mode theory, the electric field $\mathcal{E}(\mathbf{r})$ propagating along the waveguides can be presented as a superposition of the waveguide modes, $\mathcal{E}(\mathbf{r}) = \sum_{\mathbf{n}} \mathcal{E}_{\mathbf{n}} \phi(\mathbf{r} - \mathbf{n})$, where $\mathcal{E}_{\mathbf{n}}$ is the amplitude of the (single) guide mode $\phi(\mathbf{r})$ centered on site with the

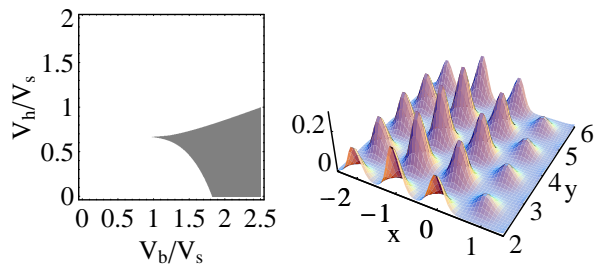


Fig. 2. (Color online) Linear interface localized modes. (a) Existence diagram with the shaded area for the modes centered at the interface. Right: Example of a linear localized mode for $V_b/V_s = 2$, $V_h/V_s = 0.5$. Square lattice ends at $x = -1$ while triangular lattice starts at $x = 0$.

lattice number $\mathbf{n} = (n_1, n_2)$. The evolution equations for the modal amplitudes $E_{\mathbf{n}}$ take the form,

$$i \frac{dE_{\mathbf{n}}}{dz} + V \sum_{n_1, n_2} E_{\mathbf{m}} + \gamma |E_{\mathbf{n}}|^2 E_{\mathbf{n}} = 0, \quad (1)$$

where \mathbf{n} denotes the position of a guide center, and the coupling V takes on the values V_s (or V_h) inside the square (or hexagonal) lattice, and V_b , along the boundary between both lattices (see notation in Fig. 1). The nonlinear parameter γ is normalized to 1 (−1) for the focussing (defocussing) nonlinearity. The lattice studied in this Letter contains 96 sites with open boundary conditions.

Next, we analyze the stationary localized modes of Eq.(1) of the form $E_{\mathbf{n}}(z) = E_{\mathbf{n}} \exp(i\beta z)$, where the amplitudes $E_{\mathbf{n}}$ satisfy the nonlinear difference equations,

$$-\beta E_{\mathbf{n}} + V \sum_{n_1, n_2} E_{\mathbf{m}} + \gamma |E_{\mathbf{n}}|^2 E_{\mathbf{n}} = 0 \quad (2)$$

We start our analysis by studying the fundamental (nodeless) modes of the system (2) in the linear limit (i.e. for $\gamma = 0$) which corresponds to low input powers $P = \sum_{\mathbf{n}} |E_{\mathbf{n}}|^2$. After normalizing the lattice couplings to one corresponding to the square lattice, we are left with two independent parameters, V_h/V_s and V_b/V_s . For given values of these two parameters, we diagonalize the appropriate matrix and examine its fundamental (nodeless) mode. In general, these modes are wide and highly asymmetric in the direction perpendicular to the interface. The position of the mode center is very sensitive to the specific value of the coupling parameters. For instance, for $V_t/V_s = V_b/V_s = 1$, the mode center is shifted inside the hexagonal lattice so that the interface acts as a *repulsive potential*, preventing the light beam from crossing the interface. Thus, we observe that the lattice topology and geometry are playing an important role. We attribute this effect to the *coordination number mismatch* that can be easily compensated by changing the interactions between the waveguides in each lattice.

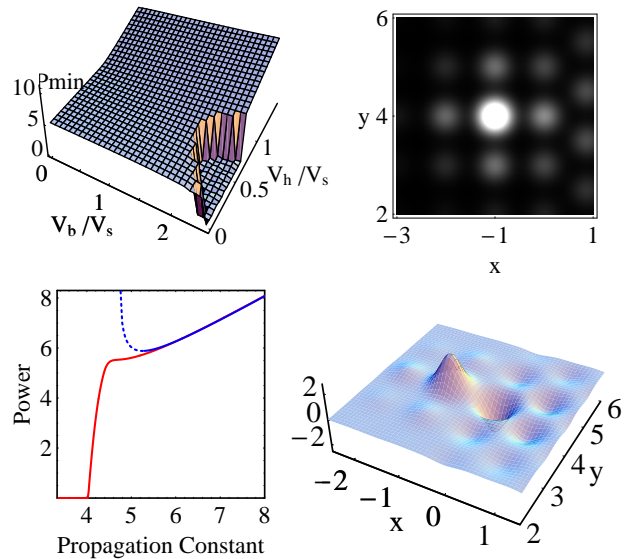


Fig. 3. (Color online) Nonlinear case ($\gamma > 0$). Top left: Minimum power to create a localized mode at the boundary of the square lattice, as a function of the couplings. Top right: Example of an interface localized mode centered on a site belonging to the boundary of the square lattice ($V_b/V_s = 1 = V_h/V_s, \beta = 5.9$). Bottom left: Power versus propagation constant for interface modes localized at the boundary of the square lattice; $V_b/V_s = 1 = V_h/V_s$ (red) and $V_b/V_s = 0.8, V_h/V_s = 1$ (blue). The dashed portion of the curve denotes an unstable regime. Bottom right: Example of a higher-order interface mode.

Indeed, if we compensate for this geometric effect by setting the ratio V_h/V_s equal to the ratio of their respective coordination numbers, $2/3$, while keeping $V_b = V_s$, *no mismatch* is observed and the resulting mode extends over both lattices.

We now make a sweep in coupling space selecting those values that lead to a mode center located at the interface either from the side of the square lattice or from the side of the hexagonal lattice. Our results are summarized in Fig. 2 in the form of a coupling-parameters diagram, along with an example of one such mode.

We move now to analyze the nonlinear interface modes of the system (i.e., $\gamma \neq 0$), looking for the low-order nonlinear modes centered at either side of the interface between the lattices. For a given value of β , we solve Eqs. (2) numerically with the help of a straightforward extension of the multidimensional Newton-Raphson method used earlier in our analysis of one-dimensional waveguide arrays [9]. We also compute the linear stability properties of each mode. Results are displayed in Figs. 1 and 3, which show some examples of low-order interface modes (Fig. 1) and the minimum power to effect an interface mode at the square side of the boundary, as a function of the coupling parameters (Fig. 3).

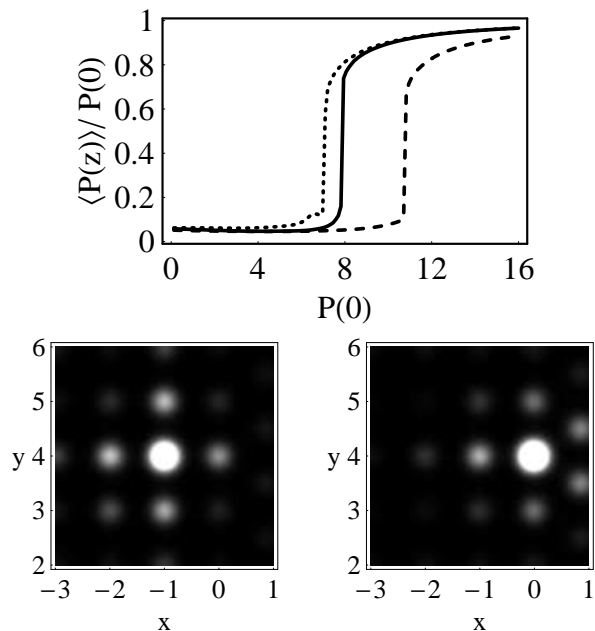


Fig. 4. Top: Average power fraction remaining at the square-triangular interface waveguide, after some propagation distance, as a function of the input power (solid). The dotted(dashed) curves refer to the cases of fully-square (triangular) lattices. ($V_b/V_s = 1 = V_t/V_s, z_{max} = 20/V_s$). Bottom: Dynamical excitation of an interface localized mode. Left: localized mode at the boundary of the square lattice. Right: Localized mode at the boundary of the triangular lattice ($V_b/V_s = 1, V_t/V_s = 2/3$, input power: 2.6). Triangular lattice starts at $x = 0$.

The presence of a steep “hole” in the power surface is due to the existence of linear interface modes (Fig. 2). The figure also shows an example of such a mode, which is substantially narrower than its linear counterpart. The stability analysis shows that all nonlinear modes originating from linear ones are always stable, while nonlinear modes outside the linear “hole” in the coupling space require a minimum power to exist. For the latter, the Vakhitov-Kolokolov stability criterium seems to hold. Finally, in Fig.3 we also show for completeness, an example of a high-order nonlinear mode, characterized by having positive amplitudes inside the square sector, while inside the hexagonal lattice the amplitudes are all negative. It could be described as a “twisted” mode along the direction perpendicular to the boundary.

Finally, we examine the dynamical excitation of a localized interface mode, excited by a highly-localized input beam launched at a boundary waveguide. As expected, for given values of V_b/V_s and V_h/V_s , a narrow state is created above some minimum power level. Figure

4 shows the average power remaining at an initial waveguide located at the very boundary between the square and triangular lattices ($V_b/V_s = 1 = V_h/V_s$), as a function of the input power. Not surprisingly, the power curve falls between the curves for the fully-square and fully-triangular lattices; with the fully-square lattice possessing the smallest threshold power for self-trapping due to its lower coordination number. Figure 4 also shows two examples of dynamically generated interface modes.

In conclusion, we have studied localization of light at the interface separating square and hexagonal photonic lattices and determined the conditions for the existence of localized surface states due to symmetry breaking. We have analyzed the effect of the lattice topology and intersite couplings on the stability of two-dimensional surface solitons which are found to differ substantially from the one-dimensional discrete surface solitons.

This work was supported by Fondecyt grant 1080374 and by the Australian Research Council.

References

1. K.G. Makris, J. Hudock, D.N. Christodoulides, G. Stegeman, O. Manela, and M. Segev, *Opt. Lett.* **31**, 2774 (2006).
2. R.A. Vicencio, S. Flach, M.I. Molina, and Yu.S. Kivshar, *Phys. Lett. A* **364**, 274 (2007).
3. H. Susanto, P.G. Kevrekidis, B.A. Malomed, R. Carretero-González, and D.J. Franzesekakis, *Phys. Rev. E* **75**, 056605 (2007).
4. X. Wang, A. Bezryadina, Z. Chen, K.G. Makris, D.N. Christodoulides, and G.I. Stegeman, *Phys. Rev. Lett.* **98**, 123903 (2007).
5. A. Szameit, Y.V. Kartashov, F. Dreisow, T. Pertsch, S. Nolte, A. Tünnermann, and L. Torner, *Phys. Rev. Lett.* **98**, 173903 (2007).
6. A. Szameit, Y. V. Kartashov, V.A. Vysloukh, M. Heinrich, F. Dreisow, T. Pertsch, S. Nolte, A. Tünnermann, F. Lederer, and L. Torner, *Opt. Lett.* **33**, 1542 (2008).
7. K.G. Makris, S. Suntsov, D.N. Christodoulides, G.I. Stegeman, and A. Haché, *Opt. Lett.* **30**, 2466 (2005).
8. S. Suntsov, K.G. Makris, D.N. Christodoulides, G.I. Stegeman, A. Haché, R. Morandotti, H. Yang, G. Salamo, and M. Sorel, *Phys. Rev. Lett.* **96**, 063901 (2006).
9. M. Molina, R. Vicencio, and Yu. S. Kivshar, *Opt. Lett.* **31**, 1693 (2006).
10. A. Szameit, Y.V. Kartashov, F. Dreisow, M. Heinrich, V.A. Vysloukh, T. Pertsch, S. Nolte, A. Tünnermann, F. Lederer, and L. Torner, *Opt. Lett.* **33**, 663 (2008).